Atomically Sharp Interlayer Stacking Shifts at Anti-phase Grain Boundaries in Overlapping MoS_2 Secondary layers

Si Zhou[1], Shanshan Wang[1,2], Zhe Shi[3], Hidetaka Sawada[4], Angus I. Kirkland[1,5], Ju Li[3,6], Jamie H. Warner[1]*

[1]Department of Materials, University of Oxford, 16 Parks Road, Oxford, OX1 3PH, United Kingdom

[2]Science and Technology on Advanced Ceramic Fibers & Composites Laboratory, National University of Defense Technology, Changsha 410073, Hunan Province, China

[3]Department of Materials Science and Engineering, MIT, 77 Massachusetts Ave, Cambridge, MA 02139, USA

[4]JEOL Ltd., 3-1-2 Musashino, Akishima, Tokyo 196-8558, Japan

[5]Electron Physical Sciences Imaging Center, Diamond Light Source Ltd, Didcot, UK

[6]Department of Nuclear Science and Engineering, MIT, 77 Massachusetts Ave, Cambridge, MA 02139, USA

Email: *Jamie.warner@materials.ox.ac.uk

Supporting Information

S1. ADF-STEM images of monolayer- bilayer interfaces

A bilayer region with an antiphase boundary is shown in Figure S1a. Two distinct stacking sequences with the boundary as interface can be identified by their unique contrast. The colored boxed regions showing the step edges are magnified in Figure S1b and c, respectively. Boxed line profile are taken along different directions for each step edge. Based on our previous experimental images and

Multislice simulation results, the atomic arrangements are displayed in Figure S1d and e to confirm that bilayer regions in Figure S1b and c are 2H and 3R stacked, respectively.

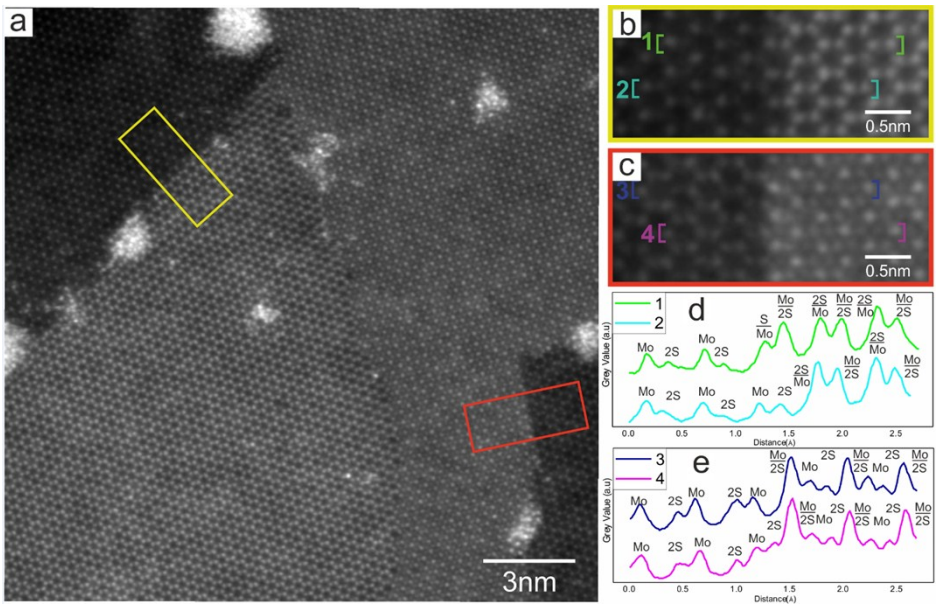

Figure S1. (a) ADF-STEM image showing the antiphase boundary propagating through a bilayer region. Two types of mono-bilayer interfaces are observed. (b and c) zoomed in images of the boxed regions in a. (d and e) Boxed line intensity profile along directions in b and c, respectively.

S2. Measurement of lattice distortion along zigzag and armchair directions

Figure S2a shows the same image we use for 4-fold ring column distance measurements in Figure 3. To take the lattice distortion, which happens due to local strain or coma and 2-fold astigmatism introduced in the image, into consideration, we conduct boxed line intensity profiles along the zigzag (direction 1) and armchair (direction 2) directions and display the results in Figure S2b and c, respectively. The average Mo-Mo distance along direction 1 is calculated as 0.313nm, exhibiting 0.95% shrinkage compared with the value in pristine MoS_2 (0.316nm). Similarly, the Mo-Mo distance along direction 2 is 0.555nm which is 1.4% higher than the standard value (0.547nm). Therefore, all measurements conducted in Figure 3 are normalized using the standard values as references.

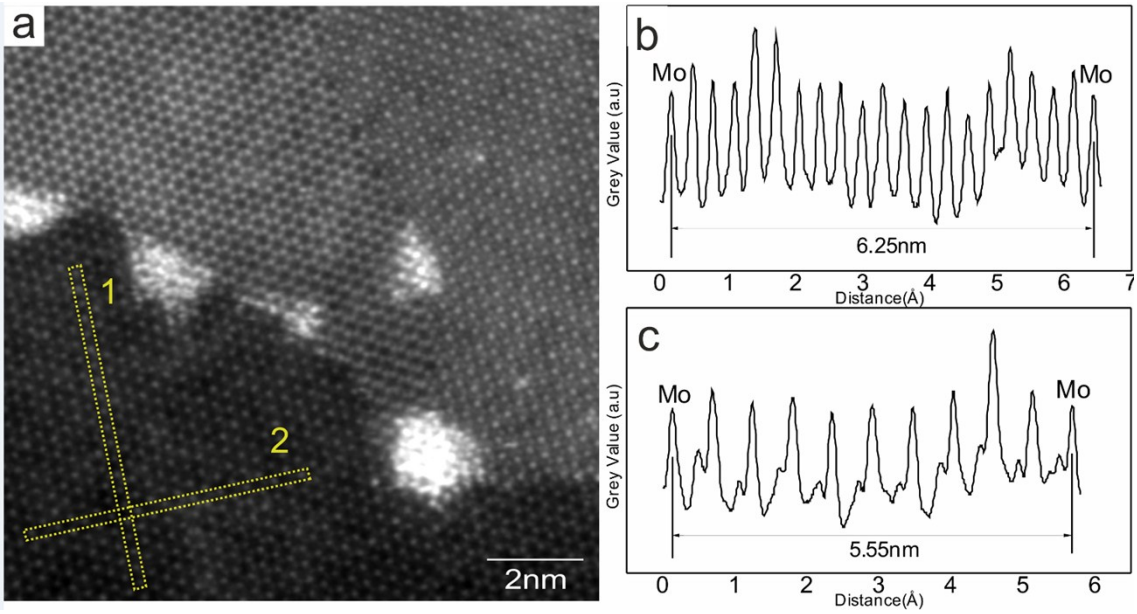

Figure S2. (a) The ADF-STEM image used for column distance measurement in Figure 3. (b and c) Boxed line intensity profile along direction 1 and 2, respectively.

S3. Dynamics of dislocation cores of the antiphase boundary in MoS_2 monolayers

Image frames in Figure S3 show local motif change during 6s under electron beam irradiation. The overlaid atomic structures in Figure S3a and d reveal that the structure only happens in the local 6-, 4- and 8- rings without affecting the propagation direction of the antiphase grain boundary. The 6-4-8 motif simply swaps to 8-4-6 motif. Based on the atomic models in Figure S3e-f, the reconstruction happens when one Mo atom is knocked out from position 1 and refills in position 2. It could also happen when Mo at position 1 migrates to position 2 along the armchair direction.

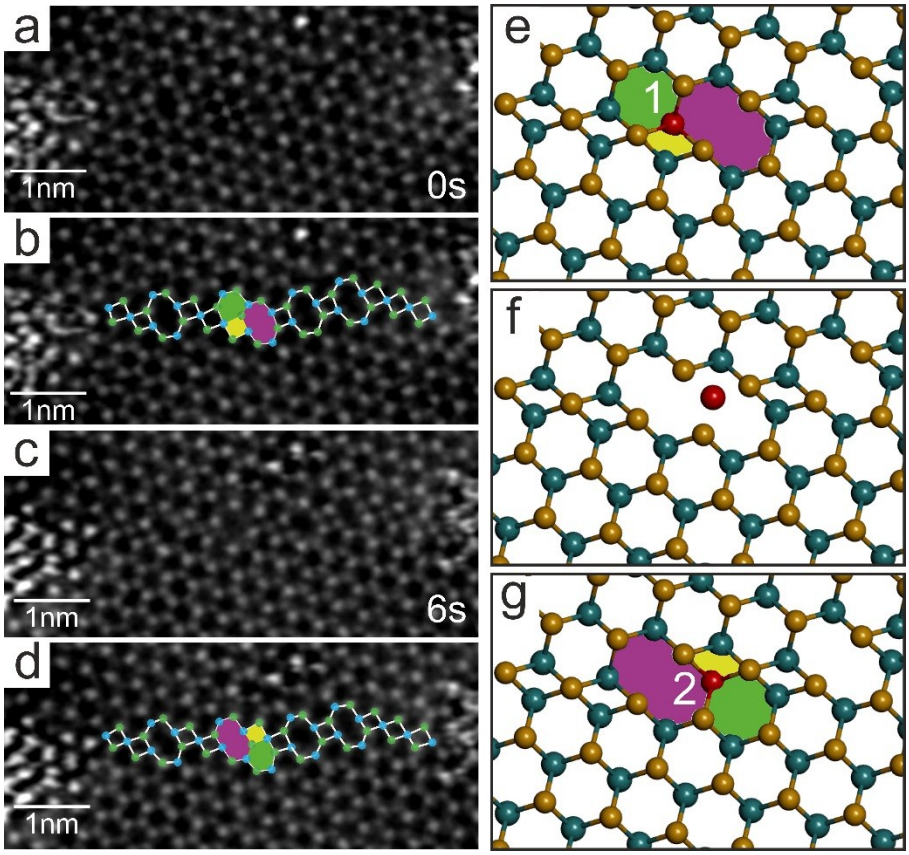

Figure S3. ADF-STEM images showing the same GB area at (a) 0s and (c) 6s. (b and d) image a and c with overlaid atomic structures, respectively, showing different local motif. (e-g) Atomic model of a single Mo atom escaping from position 1 and reappears in position 2.